Off-the-Shelf OFDM-ISAC System with Clustering Algorithm for Multipath Environments

Ha-Eun Lee*, Young-Seok Lee*, and Bang Chul Jung†
*Department of Artificial Intelligence Covergence Network, Ajou University, Suwon, 16499, South Korea
†Department of Electrical and Computer Engineering, Ajou University, Suwon, 16499, South Korea
Email: haeun.wicl@gmail.com, wiclyslee@gmail.com, bcjung@ajou.ac.kr

***Abstract*—Recently, integrated sensing and communication (ISAC) techniques have gained significant attention due to their ability to simultaneously perform sensing, localization, and communication using shared wireless resources and signal waveforms, thereby enhancing spectral and cost efficiency. Orthogonal frequency division multiplexing (OFDM) is also expected to remain a key technology in next-generation mobile communication systems due to its robustness against multipath fading and its strong support for high data rates. Building on these points, we propose a novel orthogonal sequence (OS)- based OFDM-ISAC technique fully compatible with conventional OFDM-based communication systems. This technique intelligently exploits the autocorrelation properties of OSs and the spectral efficiency of index modulation while incorporating a clustering algorithm to address challenges in multipath environments. Extensive computer simulations verify that the proposed OFDM-ISAC system delivers reliable communication and localization performance in realistic multipath environments, even in the absence of a line-of-sight (LOS) link.**

***Index Terms*—6G, Orthogonal frequency division multiplexing (OFDM), Integrated sensing and communication (ISAC), Wireless localization, Orthogonal sequence.**

I. INTRODUCTION

At the 2023 International Telecommunication Union-Radio (ITU-R) meeting, the International Mobile Telecommunication (IMT) 2030 framework was released, which outlines usage scenarios and key performance indicators for next-generation mobile communication systems [1]. Among these, the Integrated Sensing and Communication (ISAC) system, which simultaneously supports diverse functions using the same radio resources and waveforms, has emerged as a key usage scenario for sixth-generation (6G) mobile communications [2], [3].

Specifically, the ISAC system enables the concurrent support of communication and sensing functionalities within the same frequency band and hardware. It achieves target detection and localization using communication signals or, alternatively, transmits information through radar signals [4]. In [5], the authors proposed a joint subcarrier and power allocation technique for uplink OFDM-ISAC systems that communicate with the base station (BS) and detect adjacent targets simultaneously. In [6], a novel ISAC system employing successive interference cancellation (SIC) has been proposed, where the frequency band is partially shared between communication and sensing functionalities to enhance system efficiency. In [7], a transmit beamforming technique has been introduced for downlink ISAC systems, wherein a base station (BS) equipped with a uniform linear array (ULA) simultaneously transmits combined information-bearing signals and dedicated radar signals to facilitate both multiuser communication and radar target sensing in the downlink. However, conventional ISAC systems may face compatibility challenges with traditional communication systems, as they typically rely on time-frequency separation or require additional receiver structures to perform communication and sensing functions simultaneously.

Meanwhile, orthogonal frequency division multiplexing (OFDM) is anticipated to be a key technology in next-generation communication systems due to its robustness against multipath fading and its efficient support for high data rates [8]. In particular, OFDM-based communication systems operating in high-frequency bands, expected to be utilized due to the scarcity of frequency resources, have created new opportunities to deploy ISAC services [9]. In cell-free massive multiple-input multiple-output (MIMO) systems, an ISAC technique has been proposed to enable simultaneous communication and localization for a single terminal by utilizing signals received from multiple access points [10]. In [11], an OFDM-ISAC system capable of estimating the channel and angle of arrival (AoA) of each multipath component has been proposed, utilizing the preamble for this purpose. However, this may necessitate the additional integration of sensing functionality into conventional OFDM communication systems. In [12], an OFDM-ISAC algorithm for massive MIMO has been proposed to enhance channel estimation accuracy in a local scattering channel environment without a line-of-sight (LOS) path, utilizing the preamble transmitted by the user.

Unlike existing OFDM-ISAC studies that incorporate a sensing function into conventional communication systems, we consider an ISAC system that supports both communication and sensing functions simultaneously using a *single* signal waveform during the communication process between a single user equipment (UE) and the base station (BS). Moreover, although many studies assume the presence of an LOS path when supporting sensing services such as localization, this assumption may be impractical, particularly in communication environments that utilize high-frequency bands. Therefore, this paper proposes a novel OFDM-ISAC system capable of simultaneously detecting data and estimating the location of the UE during the uplink communication process using

979-8-3503-6836-9/25/$31.00 ©2025 IEEE

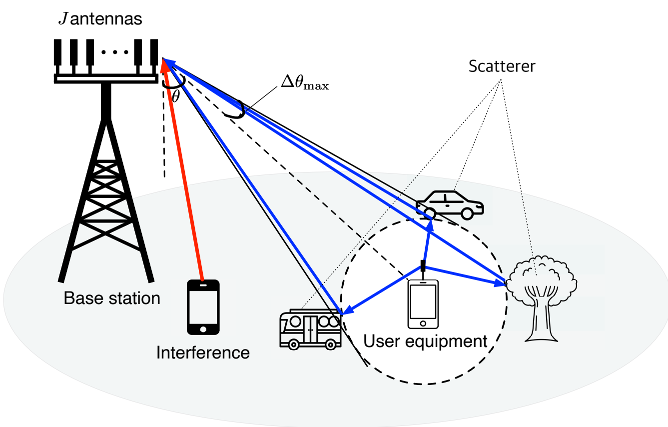

Fig. 1. System model of the proposed OFDM-ISAC system consisting of a single UE and a single BS with ULA.

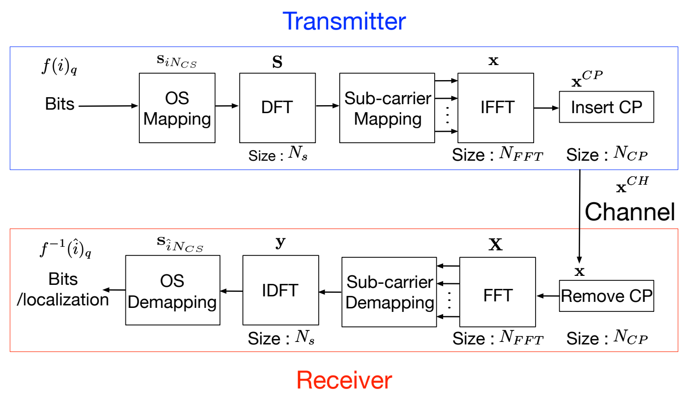

Fig. 2. Overall transmission and reception procedures of the proposed OFDM-ISAC system.

an orthogonal sequence. Additionally, we employ a local scattering channel model to represent a practical channel environment, enabling localization even in the absence of an LOS link, as demonstrated in [12]. Specifically, we consider index modulation for orthogonal sequences (OS), where the UE transmits sequences corresponding to the information bits to the BS. The BS, equipped with multiple antennas, then performs direction finding and distance estimation by leveraging the OS's autocorrelation properties. Finally, to enhance the performance of the proposed method, we further incorporate a density-based clustering algorithm [13], using the estimated distance, AoA, and power as features. Through extensive computer simulations, we verify the communication and localization performance of our proposed OFDM-ISAC technique in terms of bit-error rate (BER) and root mean squared error (RMSE), respectively.

II. System Model of OFDM-ISAC

As illustrated in Fig. 1, we consider an uplink OFDM-ISAC system consisting of a single BS that is equipped with uniform linear array antennas (ULA) having J elements and a UE with a single antenna. We assume that the BS is located at $(0,0)$ on the $x-y$ plane, and the UE is located at $(d_0 \cos\theta, d_0 \sin\theta)$. Here, d_0 represents the distance between the UE and BS, and θ denotes the angle of the UE to the x axis relative to the BS. In this paper, we also consider the local scattering channel model where most of the multipath signals are dominated by scatterers near the UE [14]. So, we assume a channel environment with no line-of-sight path component but L locally scattered multiple paths and a few external interference or general multipath components originating from arbitrary directions. Additionally, we assume that perfect time synchronization between BS and UE is achieved using techniques such as [15].

In this paper, we design an OFDM-ISAC system in which the UE transmits OS to enable the BS to estimate the UE's communication and location. Theoretically, when transmitting an orthogonal sequence with length N_s, $\lfloor \log_2 N_s \rfloor$ bits can be mapped to sequence indices. However, considering propagation delay and delay spread, it is necessary to generate candidate sequences by spacing them out to some extent rather than mapping bits to all sequences. Accordingly, by cyclically shifting sequence $\mathbf{s}_0$ by the length of N_{CS}, $Q = 2^q$ candidate sequences for $q = \lfloor \log_2 \lfloor N_s/N_{CS} \rfloor \rfloor$-bit mapping can be generated as

$$S = \left\{ \mathbf{s}_0, \mathbf{s}_{N_{CS}}, \cdots, \mathbf{s}_{(Q-1)N_{CS}} \right\}. \tag{1}$$

Moreover, we define a function $f(i)_q$ that converts an arbitrary integer $i \in \{0, \cdots, Q-1\}$ into a binary number of q-bits, then the set of q bits, B, is given by

$$B = \{f(0)_q, f(1)_q, \cdots, f(Q-1)_q\}. \tag{2}$$

For example, assuming that the $f(\cdot)_q$ function converts a decimal number to a binary number, if the integer 10 is input for 6-bit transmission, then $f(10)_6 = [001010]$.

The overall system procedure of the proposed technique is shown in Fig. 2. For ease of explanation, we describe the proposed OFDM-ISAC system in which the UE transmits the i-th candidate sequence, i.e., $\mathbf{s}_{iN_{CS}}$, to the BS. Therefore, we consider that the UE transmits $b (= f(i)_q)$ to the BS by sending $\mathbf{s}_{iN_{CS}}$. First, the transmitted OS signal defined in the time domain undergoes a discrete Fourier transform (DFT) of size N_s for OFDM subcarrier mapping. Afterwards, the frequency domain sequence signal $S(k)$ on the k-th subcarrier, whrer $k \in \{0, \cdots, N_s\}$, is as follows

$$S(k) = \sum_{n=0}^{N_s-1} \mathbf{s}_{iN_{CS}}(n) e^{-j\frac{2\pi k}{N_s}n}. \tag{3}$$

Then, the UE performs inverse fast FT (IFFT) of size N_{FFT}, larger than N_s. Here, the subcarriers corresponding to the difference between the FFT size and N_s are zero-padded. The transmit OS signal $x(m)$ after IFFT corresponding to the m-th index in the time domain, where $m \in \{0, \cdots, N_{FFT}-1\}$, can be represented as

$$x(m) = \frac{1}{N_{FFT}} \sum_{k=0}^{N_{FFT}-1} S(k) e^{j\frac{2\pi k}{N_{FFT}}m}. \tag{4}$$

Subsequently, a cyclic prefix (CP) of length N_{CP} is inserted into (4) as

$$x^{CP}(u) = x\left[(u - N_{CP}) \mod N_{FFT}\right], \tag{5}$$

where $x^{CP}(u)$ denotes u-th time domain, where $u \in \{0, \cdots, N_{FFT} + N_{CP} - 1\}$, transmit signal from the UE, and mod denotes the modulo operator.

In the p-th time, where $p \in \{0, \cdots, N_{FFT} + N_{CP} + L\}$, the received signal considering l-th multipath and propagation delay τ_j from the UE to the BS's j-th antenna can be expressed as

$$x_{l,j}^{CH}(p) = \sum_{l=0}^{L-1} \sqrt{d_l^{-\alpha}} h_j[l] x^{CP}\left[p - l - \tau_j\right] + z_j(p), \tag{6}$$

where $h_j(l)(\in \mathbb{C})$, and $z_j(p)(\in \mathbb{C})$ denote the delay-domain wireless channel for l-th multipath of j-th antenna, and time-domain additive white Gaussian noise, respectively. Also, d_l and α are the distance of l-th path from the UE to the BS and path loss exponent, respectively. In this paper, we consider a local scattering channel model for each multipath component, so that when the signal arrives at the receiving ULA, it has an angular spreading as $\theta + \Delta\theta_l$, where $\theta \in [-\pi/2, \pi/2]$ is an AoA of LoS path component and $\Delta\theta_l \in [-\Delta\theta_{max}, \Delta\theta_{max}]$ denotes angle deviation of l-th multipath component [14]. Therefore, the wireless channel of l-th multipath between the UE and j-th antenna of the BS can be defined as $h_j(l) = \beta_l e^{-j\frac{2\pi}{\lambda}(j-1)r\cos(\theta+\Delta\theta_l)}$. Here, λ denotes wavelength, r is the antenna spacing, and β_l is the complex channel gain. If the propagation delay is less than the CP length, the CP-removed signal $x_{l,j}(t)$ in t-th time index, where $t \in \{0, \cdots, N_{FFT} - 1\}$, can be expressed as

$$x_{l,j}(t) = \sqrt{d_l^{-\alpha}} h_j(l) \circledast x\left[(t - l - \tau_j) \bmod N_{FFT}\right] + z_j(t), \tag{7}$$

where $\circledast$ means circular convolution operator. By performing FFT on the received signal $x_{l,j}$, the frequency-domain received signals can be obtained as

$$\begin{aligned} &X_j(\omega) \\ &= \begin{cases} H_j(\omega)X(\omega) \cdot e^{-j\frac{2\pi\omega}{N_{FFT}}\tau_j} + Z_j(\omega), & 0 \le \omega \le N_s - 1, \\ \mathrm{FFT}\left(x_{l,j}(\omega)\right), & \omega > N_s - 1. \end{cases} \end{aligned} \tag{8}$$

Here, $H_j(w)$ and $Z_j(w)$ represent the results of performing the FFT of size N_{FFT} on $\sqrt{d_l^{-\alpha}} h_j(l)$ and z_j, respectively. In (8), due to the effect of zero-padding, the FFT results on $w > N_s - 1$ are unrelated to the transmit sequence and have negligible small values. To estimate the transmitted sequence index and distance, the BS performs an IDFT of size N_s on $X_j(\omega)$ for $0 \le \omega \le N_s - 1$. Then, the received signal $y_j(n)$ at the n-th time-domain index, where $n \in \{0, \cdots, N_s - 1\}$, can be approximated as

$$y_j(n) \approx \tilde{h}_j(n) \circledast s_{iN_{CS}}\left(n - \left\lfloor \frac{N_s}{N_{FFT}} \tau_j \right\rfloor\right) + \tilde{z}_j(n), \tag{9}$$

where $\tilde{h}_j$ and $\tilde{z}_j$ denote the IDFT results of size N_s for H_j and Z_j, respectively. The detailed derivation of (9) can be developed as in (10) at the top of the next page.

III. Sequence-Based OFDM-ISAC System

In this section, we describe the proposed OFDM-ISAC technology that detects the bits transmitted by the UE through the OS using the received signal (9) and estimates the direction and distance for calculating the UE's location. The proposed technique utilizes the autocorrelation characteristics of OS and a clustering algorithm to improve resolution. Hence, the BS first calculates the correlation profile between the received signal and OS at the $\kappa \in \{0, \ldots, N_s - 1\}$ lag as follows

$$R_j(\kappa) = \sum_{n=0}^{N_s-1} y_j(n) {s_0}^*(\kappa + n). \tag{11}$$

As mentioned earlier, using (11), the BS performs communication and wireless localization functions through three procedures: Sequence detection & demodulation, distance and direction estimation, and clustering to improve resolution.

A. Sequence Detection & Demodulation

Despite considering the OS, the correlation value may not peak at the index corresponding to the exact propagation delay due to the rounding effect caused by the size difference between the DFT and FFT in (9). We believe estimating the delay corresponding to the index with the maximum correlation value is reasonable. It is worth noting that estimating a propagation delay that is not perfectly accurate does not significantly affect sequence detection in terms of communication since we consider sequence candidates spaced apart by considering propagation delay and delay spread. Therefore, for the index $\hat{\kappa}_j = \max_\kappa R_j(\kappa)$ with the maximum correlation value, the transmitted sequence index can be detected as follows

$$\hat{i}_j = \left\lfloor \frac{\hat{\kappa}_j}{N_{CS}} \right\rfloor. \tag{12}$$

Since the BS has multiple antennas, each antenna's sequence detection results may differ. Therefore, the final sequence detection $\hat{i}$ can be determined as the mode (highest frequent index) for all antennas to obtain spatial diversity. Finally, the transmitted signal and bits from the UE are then demodulated as

$$\hat{\mathbf{s}} = \mathbf{s}_{\hat{i}N_{cs}}, \; \hat{b} = f^{-1}(\hat{i})_q, \tag{13}$$

where $f_q^{-1}(i)$ denotes the inverse function of $f_q(i)$.

B. Distance and Direction Estimation

The difference between $\hat{\kappa}_j$ and $\hat{i}_j$ can be interpreted as the transmission signal being delayed as affected by propagation delay and noise. Therefore, based on (9), the estimated distance between the BS's j-th antenna and UE can simply be calculated as

$$\hat{d}_{\hat{\kappa}_j} = c \cdot T_s \cdot \frac{N_{FFT}}{N_s} \cdot \left(\hat{\kappa}_j - \hat{i}_j\right), \tag{14}$$

$$\begin{aligned} y_j[n] &= \frac{1}{N_s}\sum_{\omega=0}^{N_s-1} H_j[\omega]X[\omega]\cdot e^{-j\frac{2\pi\omega}{N_{FFT}}\tau_j}\cdot e^{j\frac{2\pi\omega}{N_s}n}+\tilde{z}_j(n) \\ &\approx \frac{1}{N_s}\sum_{\omega=0}^{N_s-1} \mathrm{DFT}\left[\tilde{h}_j[n]\circledast\tilde{x}\left[n-\left\lfloor\frac{N_s}{N_{FFT}}\tau_j\right\rfloor\right]\right]_{N_s}\cdot e^{j\frac{2\pi\omega}{N_s}n}+\tilde{z}_j(n) \\ &= \mathrm{IDFT}\left[\mathrm{DFT}\left[\tilde{h}_j[n]\circledast\tilde{x}\left[n-\left\lfloor\frac{N_s}{N_{FFT}}\tau_j\right\rfloor\right]\right]_{N_s}\right]_{N_s}+\tilde{z}_j(n) \;= \tilde{h}_j[n]\circledast s_{iN_{CS}}\left(n-\left\lfloor\frac{N_s}{N_{FFT}}\tau_j\right\rfloor\right)+\tilde{z}_j(n) \end{aligned} \tag{10}$$

where c is the speed of light and T_s is the sampling time related to system bandwidth.

Then, we can adopt various array antenna-based direction-finding algorithms to estimate an AoA between the BS and UE, i.e., θ. Among them, the correlation method is known to be optimal in terms of RMSE according to the Cauchy-Schwarz inequality as an array antenna-based direction-finding algorithm for a single signal source. Hence, using the estimated delay index $\hat{\kappa}_j$ for each antenna, we can obtain the despreading signal $\mathbf{y}_{des,\hat{\kappa}}(\in\mathbb{C}^J)$ in the spatial domain. Here, the j-th element of $\mathbf{y}_{des,\hat{\kappa}}$ can be obtained by correlating the time-domain received signal vector $\mathbf{y}_j(=[y_j(0)y_j(1)\cdots y_j(N_s-1)]^T)$ with the sequence corresponding to the estimated index as

$$\mathbf{y}_{des,\hat{\kappa}}(j)=\mathbf{s}_{\hat{\kappa}_j}^H\mathbf{y}_j. \tag{15}$$

And then, correlating each column in a spatial dictionary (or called sensing matrix) $\mathbf{A}(\in\mathbb{C}^{J\times P})$ that contains the steering vectors for P potential angles with the despreading signal, direction finding can be performed with the index (angle) corresponding to the maximum correlation value as

$$\hat{p}_{\hat{\kappa}}=\arg\max_{p\in P}\mathbf{a}_p^H\mathbf{y}_{des,\hat{\kappa}}, \tag{16}$$

where $\mathbf{a}_p(\in\mathbb{C}^J)$ is the p-th column of $\mathbf{A}$.

C. Clustering to Improve Resolution

If $\hat{\kappa}$ corresponds to the LOS path of the UE and BS, the location of UE can be estimated using (14) and (16). In this paper, however, the LoS path is not guaranteed. We assume a local scattering channel model with numerous scatterers around the UE, necessitating additional resolution enhancement techniques for precise localization. Furthermore, if external interference has higher power than that of the UE, it may lead to significant errors in localization performance.

Therefore, this paper exploits a clustering algorithm to precisely estimate the distance and direction between the UE and BS. Specifically, the proposed technique does not distinguish the direction and distance of multiple sources but rather groups only the desired elements and treats the rest as noise. Hence, we adopt a well-known density-based clustering algorithm, the density-based spatial clustering of applications with noise (DBSCAN) algorithm [13], to more precisely estimate the direction and distance of the desired locally scattered UE signal. Briefly, the DBSCAN algorithm requires the specification of two parameters: a radius ϵ, which defines the neighborhood around each point, and ζ, which is the minimum number of points required to form a cluster. In other words, the DBSCAN algorithm can group several data into one cluster if there are ζ elements within a radius of ϵ, and classify the rest as noise. Fig. 3 shows an example of clustering characterized by the proposed OFDM-ISAC technology's distance, direction, and power of received data. Here, N_{CS} data can be collected using the estimated transmitted sequence index, i.e., $\hat{i}_c\left(\in\left\{\hat{i}_j,\cdots,\hat{i}_j+N_{CS}-1\right\}\right)$. The distance and direction of the signal corresponding to the $\hat{i}_c$ index are estimated using the method described in III-B.

Algorithm 1 Data Collection for the DBSCAN Technique

Input: $\hat{i}_c$, $\mathbf{Y}(\in\mathbb{C}^{N_s\times J})=[\mathbf{y}_1\cdots\mathbf{y}_J]$, $\mathbf{s}_0\in\mathbb{C}^{N_s}$, $\mathbf{A}(\in\mathbb{C}^{J\times P})$
Output: $\mathbf{D}(\in\mathbb{R}^{N_{CS}\times 3})$
for $i=1$ to N_{CS} **do**
  for $j=1$ to J **do**
    $\hat{i}_c=\hat{i}_j+i-1$
    $y_{des,j}=\mathbf{s}_{\hat{i}_c}^H\mathbf{y}_j$
    if $j=1$ **then**
      $\hat{i}_c=\hat{i}_1+i-1$
      $d_{i1}\leftarrow c\cdot T_s\cdot\frac{N_{FFT}}{N_s}\cdot\left(\hat{i}_c-\hat{i}_1\right)$
      $d_{i3}\leftarrow\left|\mathbf{s}_{\hat{i}_c}^H\mathbf{y}_1\right|^2$
    end if
  end for
  $p_i=\arg\max_{p\in P}\mathbf{a}_p^H\mathbf{y}_{des}$
  $d_{i2}\leftarrow$ The angle corresponding to the p_i column of $\mathbf{A}$
end for
Update $\mathbf{D}\leftarrow[\mathbf{d}_1\ \mathbf{d}_2\ \mathbf{d}_3]$

For the DBSCAN algorithm, the estimated distance, angle, and power for each path are stored in datasets $\mathbf{d}_1(\in\mathbb{R}^{N_{CS}})$, $\mathbf{d}_2(\in\mathbb{R}^{N_{CS}})$, and $\mathbf{d}_3(\in\mathbb{R}^{N_{CS}})$ respectively. Then, the overall algorithm for finding $\mathbf{D}(\in\mathbb{R}^{N_{CS}\times 3})=[\mathbf{d}_1\ \mathbf{d}_2\ \mathbf{d}_3]$ is given in Algorithm 1. We normalize the data points using their mean and standard deviation to perform clustering with equal weights for each axis as $\tilde{\mathbf{d}}_\gamma=(\mathbf{d}_\gamma-\mu_{d_\gamma})/\sigma_{d_\gamma}$ where μ_{d_γ} and σ_{d_γ} denote the mean and standard deviation of the

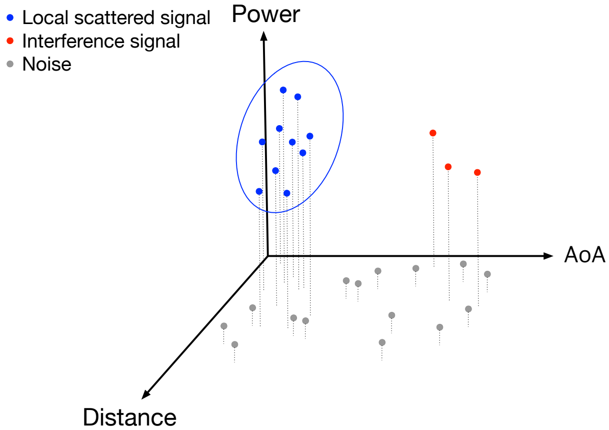

Fig. 3. An example of a data clustering algorithm featuring estimated distance, angle-of-arrival (AoA), and power in the proposed OFDM-ISAC system.

TABLE I
SIMULATION PARAMETERS

Parameter	Value	Parameter	Value
Distance between UE and BS (d_0)	40 m	Angle of arrival (θ)	45°
Center frequency (f_c)	1.8 GHz	Maximum angle deviation ($\Delta\theta_{max}$)	10°
FFT size (N_{FFT})	2048	CP size (N_{CP})	256
Threshold value (η)	1	Path loss exponent (α)	2
Number of multipath (L)	10	Number of antennas (J)	16

$\gamma(\in \{1,2,3\})$-th column of $\mathbf{D}$, i.e., $\mathbf{d}_\gamma$. In addition, in this paper, data for which the power of the normalized signal is smaller than η, the power threshold, was excluded to accelerate the clustering algorithm. After the DBSCAN algorithm, we consider the data tuple $\mathcal{V}$ within the cluster with the most pointers as $\bar{\mathbf{D}}(\in \mathbb{C}^{|\mathcal{V}|\times 3})$ associated with the desired signal, where the number of clustered data is $|\mathcal{V}|$. Finally, the distance $\hat{d}_0$ and direction $\hat{\theta}$ of the UE through the clustering algorithm can be expressed as

$$\hat{d}_0 = \min_{\nu\in\{1,\cdots,|\mathcal{V}|\}} \bar{d}_{\nu 1},\ \hat{\theta} = \frac{1}{|\mathcal{V}|}\sum_{\nu=1}^{|\mathcal{V}|} \bar{d}_{\nu 2}, \tag{17}$$

where $\bar{d}_{ij}$ refers to the element of the i-th row and j-th column of $\bar{\mathbf{D}}$.

IV. Simulation Results

This section evaluates the communication and positioning performance of the proposed OFDM-ISAC system using orthogonal sequences (OSs) through MATLAB simulations. In this study, we considered Zadoff-Chu (ZC) sequences, m-sequences, and Gold sequences, which exhibit favorable autocorrelation properties, as examples of OSs [16], [17]. Assuming that 6-bit transmission for index modulation, the ZC sequence is set to $N_s = 839$ and $N_{CS} = 13$, while the m-sequence and Gold sequence are set to $N_s = 1023$ and $N_{CS} = 15$. Additionally, Gray mapping rules for 64 phase shift keying (PSK) modulation were applied between

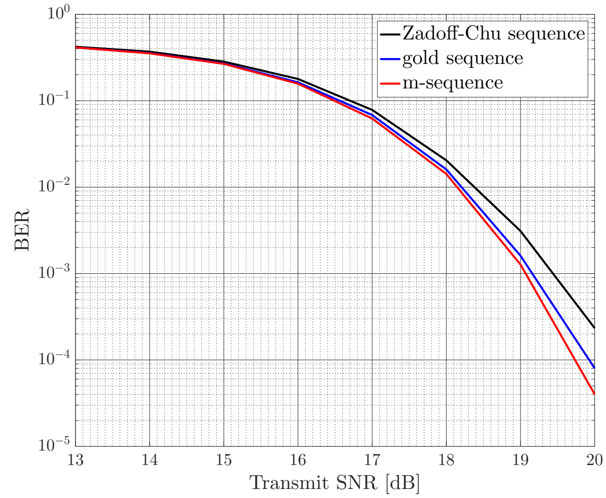

Fig. 4. BER performance of the proposed OFDM-ISAC system with various sequences.

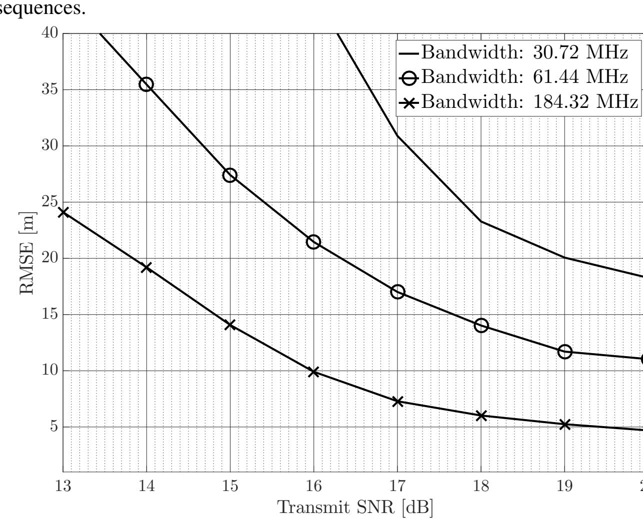

Fig. 5. RMSE performance comparison for different bandwidths in the proposed OFDM-ISAC system.

sequence indices and bits to improve the BER performance of the proposed OFDM-ISAC system. The multipath signals with L taps were considered in the local scattering channel model, and 20 percent of all taps were assumed to have external interference. For example, a delay-domain channel with $L = 10$ represents a channel environment where eight taps are produced by locally scattered multipath, while the remaining two taps are caused by external interference. As with [12], we assumed no direct LoS path exists. Several simulation parameters are summarized in Table I.

Fig. 4 shows the BER performance versus the signal-to-noise ratio (SNR) when using the three types of sequences. Here, we consider an OFDM communication system with a fixed subcarrier spacing Δf of 15 kHz and a system bandwidth of 30.72 MHz. As can be seen in Fig. 4, the ZC sequence shows a worse BER than the other sequences in all SNR ranges because the N_{CS} value set for 6-bit transmission is shorter than that of the m-sequence and the Gold sequence. On the other hand, the m-sequence, known to have better autocorrelation properties than the Gold sequence, exhibits better BER under the same N_{CS} [17]. In other words, it can be seen that the communication performance in the proposed OS-based OFDM-ISAC system is significantly affected by the N_{CS} value and the autocorrelation characteristics of the adopted OS.

Fig. 5 shows the RMSE performance for UE localization using the ZC sequence of the proposed OFDM-ISAC system for system bandwidths: 30.72 MHz for Δf=15 kHz, 61.44 MHz for Δf=30 kHz, and 184.32 MHz for Δf=90 kHz. In this paper, the RMSE for UE localization is defined as

$$\begin{aligned} &\text{RMSE} \\ &= \sqrt{\mathbb{E}\left[\left(\hat{d}_0\cos\hat{\theta} - d_0\cos\theta\right)^2 + \left(\hat{d}_0\sin\hat{\theta} - d_0\sin\theta\right)^2\right]}. \end{aligned} \tag{18}$$

To apply an efficient clustering algorithm, $5N_{CS}$ data samples for 5 received sequences are collected to precisely detect the UE's distance and direction. Note that although collecting multiple sequences, the time for an OFDM-ISAC system with a bandwidth of 30.72 MHz to acquire five sequences is only 136.76 μs when considering the sample time. In Fig. 5, it can be observed that the proposed clustering-based OFDM-ISAC system can perform localization in environments where sequence detection is successful, even without a LoS path. Furthermore, the localization performance improves with higher resolution as the system bandwidth increases, achieved by broadening the subcarrier spacing. Specifically, when the system bandwidth is 184.32 MHz, and the transmit SNR is 20 dB, the RMSE for UE localization is about 4.6 meters. In other words, it has been demonstrated that the proposed OFDM-ISAC system can ensure both communication and sensing performance using the same radio resources and hardware without requiring significant modifications to conventional OFDM system architectures.

V. Conclusion

In this paper, we have proposed an Orthogonal Frequency Division Multiplexing-based Integrated Sensing and Communication (OFDM-ISAC) system capable of simultaneously performing communication and wireless localization. The proposed system leverages index modulation and the autocorrelation properties of orthogonal sequences, allowing it to function effectively even in environments where a line-of-sight (LOS) path is not available. Through computer simulations, we have demonstrated that the proposed OFDM-ISAC system is fully compatible with conventional OFDM communication systems while ensuring robust performance in both communication and sensing tasks. As a further study, we plan to extend the proposed system to analyze its performance in scenarios involving multiple user or mobile users.

Acknowledgment

This work was supported in part by the Institute for Information and Communications Technology Planning & Evaluation (IITP) Grant funded by the Korea Government (MSIP, Development of Cube Satellites Based on Core Technologies in Low Earth Orbit Satellite Communications) under Grant RS-2024-00396992 and in part by the MSIT(Ministry of Science and ICT), Korea, under the ITRC (Information Technology Research Center) support program (IITP-2024-RS-2024-00436406) supervised by the IITP.

References

[1] S. Lu, F. Liu, F. Dong, Y. Xiong, J. Xu, and Y. -F. Liu, "Random ISAC signals deserve dedicated precoding," *IEEE Trans. Signal Process.*, vol. 72, pp. 3453–3469, Jul. 2024.

[2] Z. Wei *et al.*, "Integrated sensing and communication signals toward 5G-A and 6G: A survey," *IEEE Internet Things J.*, vol. 10, no. 13, pp. 11068–11092, Jul. 2023.

[3] Y. Wan, Z. Hu, A. Liu, R. Du, T. X. Han, and T. Q. S. Quek, "OFDM-based multiband sensing For ISAC: Resolution limit, algorithm design, and open issues," *IEEE Veh. Technol. Mag.*, vol. 19, no. 2, pp. 51–59, Jun. 2024.

[4] F. Liu, C. Masouros, A. P. Petropulu, H. Griffiths, and L. Hanzo, "Joint radar and communication design: Applications, state-of-the-art, and the road ahead," *IEEE Trans. Commun.*, vol. 68, no. 6, pp. 3834–3862, Jun. 2020.

[5] Y. Li, Z. Wei, and Z. Feng, "Joint subcarrier and power allocation for uplink integrated sensing and communication system," *IEEE Sensors J.*, vol. 23, no. 24, pp. 31072–31081, Dec. 2023.

[6] C. Zhang, W. Yi, Y. Liu, and L. Hanzo, "Semi integrated sensing and communication(semi-ISAC): From OMA to NOMA," *IEEE Trans. Commun.*, vol. 71, no. 4, pp. 1878–1893, Apr. 2023.

[7] H. Hua, J. Xu, and T. X. Han, "Optimal transmit beamforming for integrated sensing and communication," *IEEE Trans. Veh. Technol.*, vol. 72, no. 8, pp. 10588–10603, Aug. 2023.

[8] M. S. J. Solaija, S. E. Zegrar, and H. Arslan, "Orthogonal frequency division multiplexing: The way forward for 6G physical layer design?," *IEEE Veh. Technol. Mag.*, vol. 19, no. 1, pp. 45–54, Jan. 2024.

[9] C. Han, Y. Wu, Z. Chen, Y. Chen, and G. Wang, "THz ISAC: A physical-layer perspective of terahertz integrated sensing and communication," *IEEE Commun. Mag.*, vol. 62, no. 2, pp. 102–108, Feb. 2024.

[10] M. S. Herfeh, M. Kamoun, Y. Y. Chu, and S. Buzzi, "Integrated localization and communication in cell-free massive MIMO with zero over-the-air communication overhead," in *Proc. IEEE Wireless Commun. Netw. Conf. (WCNC)*, Dubai, UAE, 2024, pp. 1–6.

[11] X. Chen, Z. Feng, J. Andrew Zhang, Z. Wei, X. Yuan, and P. Zhang, "Sensing-aided uplink channel estimation for joint communication and sensing," *IEEE Wireless Commun. Lett.*, vol. 12, no. 3, pp. 441–445, Mar. 2023.

[12] K. Xu, X. Xia, C. Li, C. Wei, W. Xie, and Y. Shi, "Channel feature projection clustering based joint channel and DoA estimation for ISAC massive MIMO OFDM system," *IEEE Trans. Veh. Technol.*, Vol. 73, no. 3, pp. 3678–3689, Mar. 2024.

[13] M. Ester, H. P. Kriegel, J. Sander, and X. Xu, "A density-based algorithm for discovering clusters in large spatial databases with noise," in *Proc. KDD.*, Portland, OR, USA, 1996, pp. 226–231.

[14] E. Björnson, J. Hoydis, and L. Sanguinetti, "Massive MIMO networks: Spectral, energy, and hardware efficiency," *Found. Trends Signals Process.*, vol. 11, pp. 154–655, Nov. 2017.

[15] H. Minn, V. K. Bhargava, and K. B. Letaief, "A robust timing and frequency synchronization for OFDM systems," *IEEE Trans. Wireless Commun.*, vol. 2, no. 4, pp. 822–839, Jul. 2003.

[16] D. C. Chu, "Polyphase codes with good periodic correlation properties," *IEEE Trans. Inf. Theory*, vol. 18, no. 4, pp. 531–532, Jul. 1972.

[17] Z. Xinyu, "Analysis of M-sequence and gold-sequence in CDMA system," in *Proc. IEEE 3rd Int. Conf. Commun. Softw. Netw.*, Xi'an, China, 2011, pp. 466–468.